Chinese Chemical Letters 34 (2023) 107463

Contents lists available at ScienceDirect

Chinese Chemical Letters

journal homepage: www.elsevier.com/locate/cclet

Evaluating the pharmacokinetics of intrapulmonary administered ciprofloxacin solution for respiratory infections using *in vivo* and *in silico* PBPK rat model studies

Changzhi Shi[a], Jelisaveta Ignjatović[b], Junwei Wang[c], Yi Guo[a], Li Zhang[a], Sandra Cvijić[b,*], Dongmei Cun[a], Mingshi Yang[a,c,*]

[a] *Wuya College of Innovation, Shenyang Pharmaceutical University, Shenyang 110016, China*
[b] *Department of Pharmaceutical Technology and Cosmetology, University of Belgrade-Faculty of Pharmacy, Belgrade 11221, Serbia*
[c] *Department of Pharmacy, Faculty of Health and Medical Sciences, University of Copenhagen, Copenhagen DK-2100, Denmark*

ARTICLE INFO

Article history:
Received 27 December 2021
Revised 22 April 2022
Accepted 24 April 2022
Available online 29 April 2022

Keywords:
Inhalation antibiotics
Ciprofloxacin
Controlled release
PBPK modeling
Lung infections

ABSTRACT

Respiratory antibiotics have been proven clinically beneficial for the treatment of severe lung infections such as Pseudomonas aeruginosa. Maintaining a high local concentration of inhaled antibiotics for an extended time in the lung is crucial to ensure an adequate antimicrobial efficiency. In this study, we aim to investigate whether an extended exposure of ciprofloxacin (CIP), a model fluoroquinolone drug, in the lung epithelial lining fluid (ELF) could be achieved *via* a controlled-release formulation strategy. CIP solutions were intratracheally instilled to the rat lungs at 3 different rates, *i.e.,* T0h (fast), T2h (medium), and T4h (slow), to mimic different release profiles of inhaled CIP formulations in the lung. Subsequently, the concentration-time profiles of CIP in the plasma and the lung ELF were obtained, respectively, to determine topical exposure index (ELF-Plasma AUC Ratio, EPR). The *in silico* PBPK model, validated based on the *in vivo* data, was used to identify the key factors that influence the disposition of CIP in the plasma and lungs. The medium and slow rates groups exhibited much higher EPR than that fast instillation group. The ELF AUC of the medium and slow instillation groups were about 200 times higher than their plasma AUC. In contrast, the ELF AUC of the fast instillation group was only about 20 times higher than the plasma AUC. The generated whole-body PBPK rat model, validated by comparison with the *in vivo* data, revealed that drug pulmonary absorption rate was the key factor that determined pulmonary absorption of CIP. This study suggests that controlled CIP release from inhaled formulations may extend the exposure of CIP in the ELF post pulmonary administration. It also demonstrates that combining the proposed intratracheal installation model and *in silico* PBPK model is a useful approach to identify the key factors that influence the absorption and disposition of inhaled medicine.

Chronic lung infections are a major threat for patients, which are vitally severe with high morbidity and mortality [1-3]. Currently antibiotic management is the primary means to treat infectious diseases including respiratory infections. Most antibiotics are given *via* systemic administration such as injection and oral administration [4]. However, systemic administration of antibiotics, such as ciprofloxacin (CIP), often could not provide high antibacterial concentration in the epithelial lining fluid (ELF), causing ineffective or limited therapeutic outcomes [5,6]. Furthermore, undesired low concentration of antibiotics in the ELF, where bacteria mainly exist, can increase the risk of resistant bacteria selection [7,8]. Latterly, direct aerosolization of antibiotics to the lung was introduced as an alternative to the systemic administration with an intention to achieve high pulmonary local concentration, as well as reduced systemic side effect. Although the advantages of inhaled medicines have been well documented, the success in the development of inhaled antibiotics has been marginal, because the development of inhaled antibiotics could encounter many challenges. For instance, consideration must be given to the specific patient population, selection of infectious agents, delivery of large drug doses by inhalation, poor coherence of patients to the devices, and the patient compliance. [9,10]. Often the concentrations of inhaled antibiotics in the lung decline rapidly [11-13]. For example, the systemic exposure and pulmonary exposure showed no dis-

* Corresponding authors.
E-mail addresses: sandra.cvijic@pharmacy.bg.ac.rs (S. Cvijić), mingshi.yang@sund.ku.dk (M. Yang).

https://doi.org/10.1016/j.cclet.2022.04.061
1001-8417/

crepancy after intratracheal bolus of CIP due to high lung epithelial permeability [14]. In order to lower the permeation rate of CIP to maintain a high concentration of CIP in ELF, researchers attached metal cations (*i.e.,* Ca^{2+}, Cu^{2+}, Al^{3+}, Mg^{2+}) to CIP to form complex. In a Calu-3 cell model, their study demonstrated that the epithelial apparent permeability of CIP could be reduced. The higher the complex affinity, the lower the CIP apparent permeability [15,16]. Their subsequent study also showed that this modification of CIP could lead to a significant improvement of the CIP concentration in the ELF post intratracheal administration in a rat model [17]. The long-term application of the metal ions raises some safety concern though. Some other innovative formulations have also been attempted with an intention to extend the exposure of CIP in the lung post pulmonary administration. For example, CIP was encapsulated in liposomal formulations to provide CIP with prolonged *in vitro* drug release [18-20]. In other reports, the practically insoluble zwitterionic form of CIP was formulated into dry powders for inhalation [21,22]. Presumably, these formulations would render CIP controlled-release profiles in the lung and exert an extended pulmonary exposure [23,24]. However, up to date, few studies have been performed to verify these formulation strategies to enhance pulmonary exposure of inhaled antibiotics *in vivo*.

In this study, we used CIP as a model drug, which was delivered to the rat lungs *via* intratracheal instillation to mimic different dissolution rates (fast, medium, and slow) of CIP in the lung. Subsequently, the concentration-time profiles of CIP in the ELF and in the plasma were plotted, respectively to verify the relationship of controlled-release formulations and pulmonary exposure. Additionally, a CIP-specific *in silico* PBPK model was constructed and verified based on the *in vivo* data, and further exploited to identify the key factors that influence the absorption and disposition of CIP following different drug exposure rates to the lungs.

Ciprofloxacin hydrochloride, supplied as a dried fine powder, was reconstituted in 0.9% NaCl to prepare solution (10 mg/mL, ciprofloxacin) for administration. Male Sprague-Dawley rats (200-220 g, SPF) were supplied by Liaoning Changsheng Biotechnology Co., Ltd. (China), animal health was certified by China Medical University (SYXK Liao 20180009). All procedures were conducted under the guidelines of experimental animal center of Shenyang Pharmaceutical University and approved by the local Animal Ethics Committee (SYPUIACUCC 2020081272). The targeted dose of ciprofloxacin was 20 mg per kg body weight (4 mg/200 g, ciprofloxacin). These rats were divided into four groups (IV, T0h, T2h, T4h) and anaesthetized with inhaled ether narcosis. The intravenous bolus injection of ciprofloxacin solution (1 mL, 4 mg/mL) for IV group was performed *via* tail vein. The pulmonary groups (T0h, T2h, T4h) were respectively treated with intratracheal instillation of ciprofloxacin solution (0.4 mL, 10 mg/mL) using a highly precise pump (Longer Precision Pump Co., Ltd., Hebei, China) *via* a polyethylene catheter, and the tip of the catheter was introduced into the rat's trachea with visualization of a laryngoscope, to perform the intratracheal administrations with variable instillation duration, *i.e.* 0 h, 2 h and 4 h, respectively (Fig. 1), *via* flow rate settings of the micro-perfusion pump. Animals underwent necropsy immediately at predetermined time points (0.25, 0.5, 1, 2, 4 and 6 h) post dosing for bronchoalveolar lavage (BAL) and blood sampling. The chest cavity of rats was opened, pre-warmed saline was injected into the airways *via* a polyethylene microtube. BAL sample was immediately collected by aspiration, then centrifuged at 13800 *g* for 5 min to remove cell debris, transferred the supernatant into a new labeled vial. After that, blood samples were collected by intracardiac puncture (into micro-vacutainer) and centrifuged (13800 *g*, 5 min) to collect plasma. The lung was freshly harvested and divided into proximal, middle and distal portions, then homogenized with saline. Finally, samples were flash frozen and stored at -20 °C until analysis.

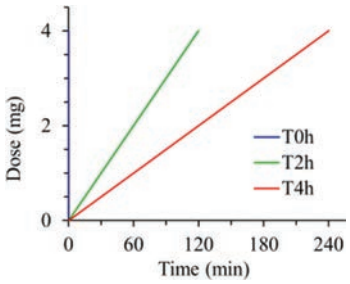

Fig. 1. Protocol for delivering ciprofloxacin to the rat lungs with diverse rates but the same drug dose (20 mg/kg). T0h-blue, T2h-red and T4h-green indicate instillation time within 2 min, 2 h and 4 h, respectively.

These samples were prepared by a protein precipitation method [25,26], as the following steps: An internal reference standard levofloxacin (0.5 μg/mL) was vortex-mixed with aliquots of 200 μL serum or 200 μL BAL. Methanol and perchloric acid solution (5% w/v) were added into the above-prepared samples and vortexed to precipitate the water-soluble proteins, along with centrifugation (13800 *g*, 10 min) to obtain the supernatant. The supernatant was filtered and then 20 μL aliquot was analyzed by the HPLC. HPLC method was carried out by Hitachi chromatographic system (Hitachi High Technologies Corporation, Tokyo, Japan) equipped with a 5410 UV-detector and Chromaster software. The HPLC analysis was performed using a BDS Hypersil C18 column (5 μm, 250 mm × 4.6 mm ID, Thermo Fisher Scientific, USA) at 30 °C and detection wavelength was 297 nm. The mobile phase was composed of methanol, acetonitrile and water mixture supplemented with 0.01 mol/L phosphoric acid and 0.5 mol/L tetrabutylammonium bromide (30:30:430:10, v/v/v/v). Isocratic elution of samples was conducted for 10 min at a flow rate of 1.0 mL/min with a retention time (5.8 min). The calibration curve was constructed by linear regression of the peak areas over the concentration range of approximately 0.2-160 μg/mL ($R^2 > 0.999$). The precision and accuracy of inter-day and intra-day precision were less than 5% for 3 quality control concentrations (10 μg/mL, 50 μg/mL, 150 μg/mL), and the limit of detection and limit of quantitation were 40 ng/ml and 200 ng/mL, respectively. For ELF concentration ($Con\text{-}_{ELF}$), it was estimated from the bronchial alveolar lavage fluid concentrations ($Con\text{-}_{BAL}$) with equation (Eq. 1), where the U was a dilution factor calculated by the urea concentration ratio of plasma with BAL [14].

$$Con\text{-}_{ELF} = Con\text{-}_{BAL} \times U \quad (1)$$

Commercial software GastroPlus™ (version 9.8.1003, Simulations Plus, Inc. USA) was used as the *in silico* modeling tool. An additional Pulmonary Compartmental Absorption & Transit (PCAT™) module in the GastroPlus™ was used to estimate drug absorption and disposition following intratracheal administration of the tested formulations. PCAT™ model was linked with Advanced Compartmental Absorption and Transit (ACAT™) model of the gastrointestinal (GI) tract to predict the absorption of the swallowed drug fraction, and they were coupled with Physiologically Based Pharmacokinetic (PBPK) model to simulate drug distribution through different tissues/organs. The selected PBPK model used GastroPlus™ default physiology parameters for rat with mean body weight of 0.2 kg. All tissues/organs were treated as perfusion-limitted. Tissue/plasma partition coefficients (K_p) were calculated using the Lukacova (modified Rodgers-Single) equation, where unbound fraction in tissue (f_{ut}) was calculated using S+ v9.5 equation. The input parameters for GastroPlus™ simulations (Table 1) were taken from literature, *in silico* estimated or experimentally determined [27-31].

Table 1
Summary of input parameters for PBPK modeling.

Parameter	Value
Molecular weight (g/mol)	331.3 [27,28]
Solubility (mg/mL)	0.1887 (pH 6.8) [28,29]
pK_a	6.16 (acid) [28]
	8.62 (base)
log*P*	1.32 [28]
Diffusion coefficient ($cm^2/s, \times 10^{-5}$)	0.75 [a]
Dose (mg)	4.00 [b]
Dosage form	intravenous bolus injection; pulmonary infusion solution
Infusion (instillation) time (h)	0, 2, and 4 [b]
Body weight (kg)	0.20 [b]
Permeability, rat jejunum ($cm/s, \times 10^{-4}$)	0.08 [27,30]
Blood/plasma concentration ratio	0.96 [31]
Fraction unbound in plasma (%)	67 [31]
Clearance (L/h)	0.65 [c]
Pulmonary solubility (mg/mL)	1.86 [a]
Pulmonary permeability (cm/s)	3.66×10^{-6} (thoracic) [a]
	6.05×10^{-6} (bronchiolar) [a]
	2.13×10^{-4} (alveolar) [a]
Pulmonary absorption rate constant, k_a (1/s)	3.206×10^{-3} [c]

[a] GastroPlus™ calculated value.
[b] Experimental value.
[c] Optimized value.

PKPlus™ module in GastroPlus™ software was used to estimate CIP pharmacokinetic parameters (noncompartmental analysis, NCA) based on the *in vivo* obtained plasma concentration-time data following intravenous drug administration to rats. The clearance value (CL) used for the simulations was optimized to best describe the drug elimination phase. Moreover, in order to match the volume of distribution (V_{ss}) calculated from the *in vivo* data, the software calculated K_p values for all organs were multiplied by factor 2.1. Experimentally obtained drug deposition data in rats' lungs (Table S1 in Supporting information) were used as inputs for the simulations. CIP pulmonary absorption rate constant was optimized to match the *in vivo* data. The predictive power of the designed model was tested by comparing the simulation outcomes with the *in vivo* data. The percent prediction error (PE%) values between the *in vivo* observed and *in silico* predicted PK parameters (C_{max}, t_{max}, $AUC_{0\text{-}inf}$, $AUC_{0\text{-}6h}$) were calculated using equation (Eq. 2). Parameter sensitivity analysis (PSA) was used to assess the influence of the selected input parameters (drug permeability and pulmonary absorption rate constant in thoracic, bronchiolar and alveolar regions) on the predicted pharmacokinetic parameters (C_{max}, t_{max} and $AUC_{0\text{-}6h}$), that describe the rate and extent of CIP absorption.

$$PE(\%) = \left(Value_{observed} - Value_{predicted}\right)/Value_{observed} \times 100\% \quad (2)$$

The obtained semi-log concentration-time pharmacokinetic profiles are illustrated in Fig. 2, and the NCA results for the pharmacokinetic parameters corresponding to the plasma and ELF concentrations are shown in Table 2.

As shown, the C_{max}, t_{max}, and MRT of IV and T0h groups in the plasma samples are very similar. This can be attributed to the high permeability of CIP molecule and the short distance between the air and the blood in the lung. In contrast, the C_{max} of T2h and T4h groups in the plasma samples are much lower than that of the IV group. This suggests that a slow instillation of CIP to the lung could retard and extend its systemic exposure. However, the overall difference of CIP in the plasma exposure (area under curves, $AUC_{0\text{-}t}$) for all groups are quite smaller than that of ELF exposure. This suggests that the systemic bioavailability of CIP post pulmonary administration would not be influenced by the alteration of the rates of the dissolution or release from the formulations. This may be attributed to the excellent tissue permeability of CIP that resulted

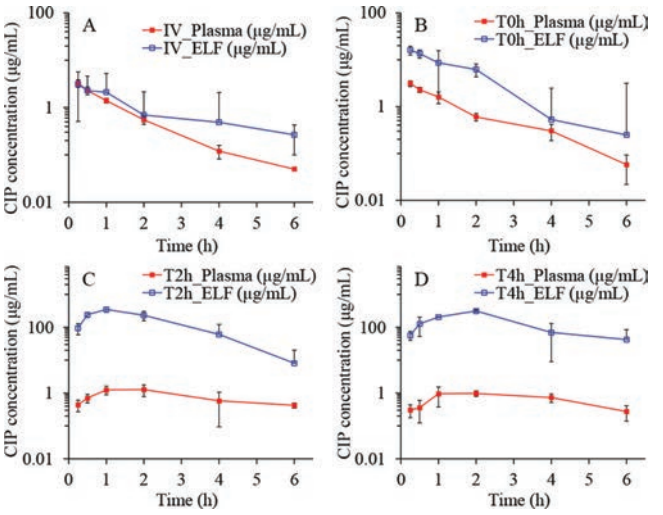

Fig. 2. Observed time-concentration profiles of CIP in plasma and lung ELF post dosing. (A) IV, injection; (B) T0h, instillation: fast rate; (C) T2h, instillation: middle rate; (D) T4h, instillation: slow rate ($n = 4$, Mean ± SD).

Table 2
Pharmacokinetic parameters of the plasma and ELF concentrations post administration by PKPlus™.

Type	IV		T0h		T2h		T4h	
	Plasma	ELF	Plasma	ELF	Plasma	ELF	Plasma	ELF
C_{max} (μg/mL)	3.28	3.10	3.10	15.99	1.28	350.43	0.98	315.43
$AUC_{0\text{-}t}$ (μg h/mL)	4.21	5.98	4.40	26.12	4.83	854.20	4.15	873.50
$AUC_{0\text{-}inf}$ (μg h/mL)	4.37	6.84	4.47	26.77	7.59	862.20	4.72	1043.40
t_{max} (h)	0.25	0.25	0.25	0.25	2.00	1.00	2.00	2.00
$t_{1/2}$ (h)	0.91	2.27	0.83	1.84	4.48	0.69	1.42	2.77
MRT (h)	1.04	2.58	1.54	1.49	5.13	0.85	1.36	1.49
CL (L h^{-1} kg^{-1})	4.58	2.92	4.48	0.75	2.64	0.02	4.24	0.02
V_{ss} (L/kg)	4.77	7.58	6.90	1.12	13.53	0.02	5.78	0.03

in fast infusion into systemic circulation regardless of the delivery routes, with less elimination to untargeted organs [13]. After 6 h, no CIP was detected in plasma for all groups, suggesting CIP is being eliminated quickly from the circulation system.

As observed from the ELF concentration-time profiles of the IV and T0h group, the concentrations of CIP in the ELF declined rapidly post administration (Figs. 2A and B). This may be attributed to a combined effect of pulmonary elimination and systemic clearance. In contrast, the ELF concentration-time profiles of the T2h and T4h groups exhibited two distinct phases, *i.e.,* an increase in CIP at an initial phase followed by a sharp decline of CIP concentration in the ELF (Figs. 2C and D). The initial increase phase of the CIP concentration-time profiles of T2h and T4h groups can be attributed to the continuous delivery of CIP into the lung. The same volume of CIP solutions was instilled to the lung with different infusion rates. The fast infusion rate might have resulted in a rapid spreading of CIP solutions into the deep airways and wider lung distribution in the lungs as compared to CIP administered with slow infusion rate.

Although the permeation of CIP to the blood is rapid, the instillation rate of CIP might control the permeation rate of CIP through the epithelium. In another words, the drug was accumulated in the ELF due to the continuous instillation of the CIP solutions to the lung.

Following this initial phase, a decline of CIP in the ELF can be observed. It should be noted that other clearance pathway such as mucociliary clearance and lymphatic circulation may have also contributed to the overall elimination process. Notably, the mean lung concentrations exhibited significant decline in the elimina-

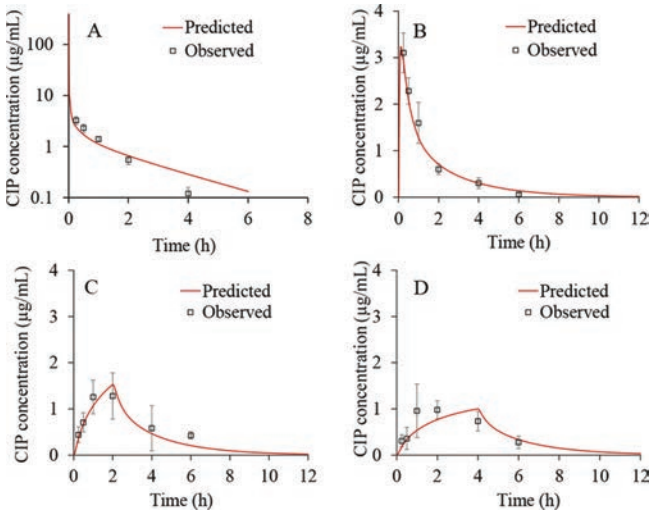

Fig. 3. Predicted and observed CIP plasma concentration-time profiles following 4 mg intravenous bolus administration (A), fast IT instillation (B), moderate IT instillation (C) and slow IT instillation (D) of 4 mg strength infusion solution.

tion phase for the groups T2h and T4h along with end-instillation and showed similar blood elimination as the groups IV and T0h. This indicates that the blood elimination behavior of CIP post pulmonary administration does not change with respect to group IV.

According to the data shown in Table 2, the highest overall exposure of CIP in the lungs was observed for the group T4h, which is followed by the T2h group. The overall lung exposure of the IV and T0h group are very low though. In contrast, interestingly, the systemic exposure of CIP from the four groups were similar. It suggests that the pulmonary exposure of CIP could be improved by slowing the instillation rate of CIP to the ELF. In addition, the findings of this study also suggest that slowing the instillation rate of CIP to the ELF could increase lung target effects of CIP (Table S2 in Supporting information). It implies that the efficacy of controlled-release CIP formulations may be improved by pulmonary administration.

To justify the selection of the input pharmacokinetic inputs, the resultant elimination half-life ($t_{1/2}$), calculated based on the selected V_{ss} and *CL*, was compared with the *in vivo* values. The model calculated $t_{1/2}$ fitted into the range of the calculated values (Table S3 in Supporting information). This value also complied with the range of 0.7-1.7 h reported in different literature sources for ciprofloxacin $t_{1/2}$ in rats [22,31-33].

The simulated CIP plasma concentration-time profiles following administration of intravenous bolus in rats, together with the *in vivo* observed values was represented in Fig. 3A. It can be observed that the simulated profile matched the *in vivo* values well. The only discrepancy concerns the predicted C_{max} (460.91 μg/mL) which was notably higher in comparison to the *in vivo* value (3.28 μg/mL), but this can be explained by the late first sampling time in the *in vivo* study (the first sample was taken after 15 min, which means that the real C_{max} value was missed). Figs. 3B-D show the predicted CIP plasma profiles following intratracheal administration of the drug solution with different instillation rates. For the fast IT instillation rate (T0h), the predicted plasma concentration-time profile matched well the shape of the *in vivo* observed profile (Fig. 3B).

In addition, Table 3 demonstrates that the predicted C_{max}, $AUC_{0\text{-inf}}$ and $AUC_{0\text{-6h}}$ closely resemble the observed ones. This was confirmed by the calculated PE, which was lower than 10%. Only the predicted t_{max} (0.12 h) diverged from the mean *in vivo* observed value (0.25 h) but since the first sampling time was 15 min, the real t_{max} may have been missed, indicating that the simulated value may be a reasonable estimate. In the case of moderate CIP IT instillation rate (T2h), the predicted plasma profile also resembled the shape of the mean *in vivo* observed profile (Fig. 3C).

Table 3
Predicted and observed pharmacokinetic parameters for CIP IT instillation (fast/moderate/slow).

Parameter	Observed mean (range)[a]	Predicted	PE (%)
T0h			
C_{max} (μg/mL)	3.10 (2.77-3.30)	3.23	-4.19
t_{max} (h)	0.25 (0.25-0.25)	0.12	52.00
$AUC_{0\text{-inf}}$ (μg h/mL)	4.47 (3.99-5.41)	4.77	-6.71
$AUC_{0\text{-6h}}$ (μg h/mL)	4.40 (3.95-4.95)	4.40	0
T2h			
C_{max} (μg/mL)	1.28 (1.14-1.78)	1.53	-19.53
t_{max} (h)	2.00 (1.00-2.00)	2.00	0
$AUC_{0\text{-inf}}$ (μg h/mL)	7.59 (4.83-10.70)	4.77	36.99
$AUC_{0\text{-6h}}$ (μg h/mL)	4.83 (4.03-5.51)	4.23	10.19
T4h			
C_{max} (μg/mL)	0.98 (0.93-1.29)	0.99	-1.02
t_{max} (h)	2.00 (1.00-2.00)	4.00	-100
$AUC_{0\text{-inf}}$ (μg h/mL)	4.72 (4.50-5.30)	4.77	-1.27
$AUC_{0\text{-6h}}$ (μg h/mL)	4.15 (3.55-4.79)	3.91	5.78

[a] The range calculated from individual profiles.

All the predicted pharmacokinetic parameters fitted into the range of individually observed values, except $AUC_{0\text{-inf}}$ which was slightly below the observed range (Table 3). The prediction results for CIP slow IT instillation rate of 4 h partly deviated from the mean *in vivo* plasma profile (Fig. 3D). Namely, according to the simulations, it can be expected that the maximum drug concentration in plasma will be achieved in 4 h, *i.e.,* when the IT instillation of CIP solution is finished. But, according to the *in vivo* data, t_{max} was achieved earlier (at 2.00 h), which can be subject to the influx/efflux transepithelial transport [10-12,19,21]. As for the other pharmacokinetic parameters (C_{max}, $AUC_{0\text{-inf}}$ and $AUC_{0\text{-6h}}$), the model predicted these values well, as demonstrated by the PE values less than 10% (Table 3).The predicted drug exposure in the whole lung tissue (not ELF), expressed as $AUC_{0\text{-6h}}$, did not show large differences depending on the CIP solution instillation rate ($AUC_{0\text{-6h}} = 466.73$ μg h/mL for T0h, $AUC_{0\text{-6h}} = 421.88$ μg h/mL for T2h, and $AUC_{0\text{-6h}} = 407.73$ μg h/mL for T4h). These data do not fully comply with the *in vivo* results showing that the drug exposure in ELF for T2h and T4h groups is notably higher than for T0h group. Such discrepancies might be explained by the fact that the *in vivo* values refer to the drug concentrations in ELF, while the simulated values represent CIP concentrations in the whole lungs. However, there was a notable difference between the predicted $AUC_{0\text{-6h}}$ value for total lung concentration-time curve following intravenous administration ($AUC_{0\text{-6h}} = 66.88$ μg h/mL) in comparison to the three intratracheal administration scenarios, which complies with the *in vivo* results.

The generated CIP-specific model was also used to test several input parameters for their influence on the rate and extent of CIP absorption following intratracheal administration in rats. According to the PSA results, pulmonary absorption rate constant in alveolar region was identified as the key parameter with the highest effect on the predicted C_{max}, t_{max} and $AUC_{0\text{-6h}}$ following CIP IT instillation (Fig. 4). The absorption rate constants in thoracic and bronchiolar regions showed minimal effect on C_{max} and $AUC_{0\text{-6h}}$ values. Also, CIP permeability through different lung regions did not affect any of the predicted pharmacokinetic parameters.

This study demonstrates that an extended exposure of ciprofloxacin (model fluoroquinolone) in the lung can be achieved *via* a controlled-release strategy in an intratracheal installation model in rats. A whole body PBPK model, established through iterative comparison between the predicted and observed results re-

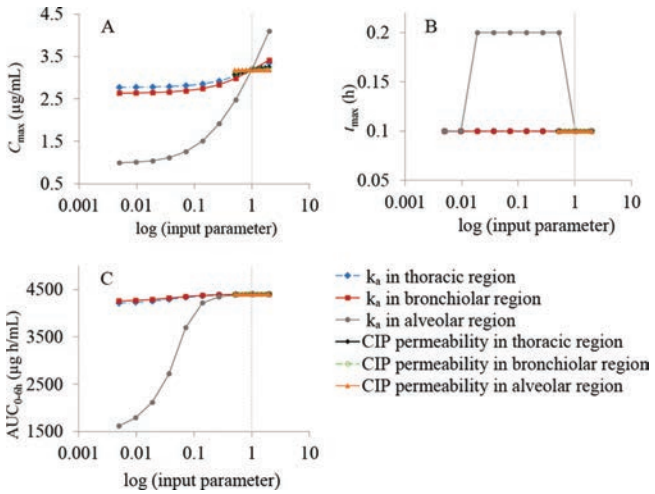

Fig. 4. PSA results for the influence of drug permeability and absorption rate constants in thoracic/bronchiolar/alveolar regions on the predicted C_{max} (A), t_{max} (B), and $AUC_{0\text{-}6h}$ (C) for fast IT instillation of CIP solution; vertical dotted lines represent the initial input values. Data for the other groups comply with these results.

vealed that pulmonary absorption rate in alveolar region has a strong ability to extend lung exposure of ciprofloxacin. The absorption rate is usually a net result of drug, formulation and physiological properties, thus inhaled medicines for lung infection are worth being developed if considering both controlled-release formulation potential and decreased lung tissue permeability (*e.g.,* due to the thick covering bacterial biofilm in the airways). Furthermore, this study suggests that combination of intratracheal installation model and *in silico* PBPK model is a useful approach to identify the key limiting factors that influence the *in vivo* disposition of inhaled drugs.

Declaration of competing interest

The authors declare that they have no known competing financial interests or personal relationships that could have appeared to influence the work reported in this paper.

Acknowledgments

This work was financially supported by the Liaoning Pan Deng Xue Zhe Scholar (No. XLYC2002061), the National Natural Science Foundation of China (No. 81573380), and the Overseas Expertise Introduction Project for Discipline Innovation ("111 Project") (No. D20029). D.Cun acknowledges financial support from the Guiding Project for Science and Technology of Liaoning Province (No. 2019-ZD-0448), and Ministry of Education Chunhui Program (2020). The authors acknowledge support from Ministry of Education Science and Technological Development, Republic of Serbia (No. 451-03-9/2021-14/200161).

Supplementary materials

Supplementary material associated with this article can be found, in the online version, at doi:10.1016/j.cclet.2022.04.061.

References

[1] Q. Zhou, S.S.Y. Leung, P. Tang, et al., Adv. Drug Deliv. Rev. 85 (2015) 83–99.
[2] J.K. Mukker, R.S.P. Singh, H. Derendorf, Adv. Drug Deliv. Rev. 85 (2015) 57–64.
[3] Y. Guo, H. Bera, C. Shi, et al., Acta Pharm. Sin. B 11 (2021) 2565–2584.
[4] P.C. Sharma, A. Jain, S. Jain, et al., J. Enzyme Inhib. Med. Chem. 25 (2010) 577–589.
[5] N. Günday Türeli, A. Torge, J. Juntke, et al., Eur. J. Pharm. Biopharm. 117 (2017) 363–371.
[6] X. Zheng, Q. Cao, Q. Cao, et al., Chin. Chem. Lett. 31 (2020) 413–417.
[7] D. Cipolla, J. Blanchard, I. Gonda, Pharmaceutics 8 (2016) 1–31.
[8] E. Gullberg, S. Cao, O.G. Berg, et al., PLoS Pathog. 7 (2011) 1–10.
[9] E. Wenzler, D.R. Fraidenburg, T. Scardina, et al., Clin. Microbiol. Rev. 29 (2016) 581–632.
[10] T. Karampitsakos, O. Papaioannou, M. Kaponi, et al., Pulm. Pharmacol. Ther. 60 (2020) 101885.
[11] J. Brillault, W.V. De Castro, W. Couet, Antimicrob. Agents Chemother. 54 (2010) 543–545.
[12] H.X. Ong, D. Traini, M. Bebawy, et al., Antimicrob. Agents Chemother. 57 (2013) 2535–2540.
[13] J.E. Hastedt, P. Bäckman, A.R. Clark, et al., AAPS Open 2 (2016) 1–20.
[14] A.V.L. Gontijo, J. Brillault, N. Grégoire, et al., Antimicrob. Agents Chemother. 58 (2014) 3942–3949.
[15] J. Brillault, F. Tewes, W. Couet, et al., Eur. J. Pharm. Sci. 97 (2017) 92–98.
[16] F. Tewes, J. Brillault, B. Lamy, et al., Mol. Pharm. 13 (2016) 100–112.
[17] B. Lamy, F. Tewes, D.R. Serrano, et al., J. Control. Release 271 (2018) 118–126.
[18] S. Yu, S. Wang, P. Zou, et al., Int. J. Pharm. 575 (2020) 118915.
[19] G. Chai, H. Park, S. Yu, et al., Int. J. Pharm. 569 (2019) 118616.
[20] I. Khatib, D. Khanal, J. Ruan, et al., Int. J. Pharm. 566 (2019) 641–651.
[21] J. Weers, Pulm. Ther. 5 (2019) 127–150.
[22] P.J. McShane, J.G. Weers, T.E. Tarara, et al., Pulm. Pharmacol. Ther. 50 (2018) 72–79.
[23] Q. Wang, L. Ge, L. Wang, et al., Chin. Chem. Lett. 32 (2021) 1071–1076.
[24] J. Du, J. Guo, D. Kang, et al., Chin. Chem. Lett. 31 (2020) 1695–1708.
[25] U. Neckel, C. Joukhadar, M. Frossard, et al., Anal. Chim. Acta 463 (2002) 199–206.
[26] S. Watabe, Y. Yokoyama, K. Nakazawa, et al., J. Chromatogr. B: Anal. Technol. Biomed. Life Sci. 878 (2010) 1555–1561.
[27] S. Hansmann, Y. Miyaji, J. Dressman, Eur. J. Pharm. Biopharm. 122 (2018) 186–196.
[28] J.F. Schlender, D. Teutonico, K. Coboeken, et al., Clin. Pharmacokinet. 57 (2018) 1613–1634.
[29] M.E. Olivera, R.H. Manzo, H.E. Junginger, et al., J. Pharm. Sci. 100 (2011) 22–33.
[30] M. Rodríguez-Ibáñez, G. Sánchez-Castaño, M. Montalar-Montero, et al., Int. J. Pharm. 307 (2006) 33–41.
[31] M.H. Park, S.H. Shin, J.J. Byeon, et al., Korean J. Physiol. Pharmacol. 21 (2017) 107–115.
[32] S. Li, Y. Yu, X. Bian, et al., Arch. Toxicol. 95 (2021) 1683–1701.
[33] B. Nouaille-Degorce, C. Veau, S. Dautrey, et al., Antimicrob. Agents Chemother. 42 (1998) 289–292.